Supporting Information

An Electric Single-Molecule Hybridisation Detector for short DNA Fragments

A.Y.Y. Loh,[1] C.H. Burgess,[2] D.A. Tanase,[1] G. Ferrari,[3] M.A. Maclachlan,[2] A.E.G. Cass,[1] T. Albrecht*[1,4]

[1]Imperial College London, Department of Chemistry, Exhibition Road, London SW7 2AZ, UK

[2]Imperial College London, Department of Materials and Centre for Plastic Electronics, London SW7 2AZ, United Kingdom

[3] Politecnico di Milano, Dipartimento di Elettronica, Informazione e Bioingegneria, P.za Leonardo da Vinci 32, Milano, Italy

[4]University of Birmingham, School of Chemistry, Edgbaston Campus, Birmingham B15 2TT, UK

*t.albrecht@bham.ac.uk

The Supporting Information provides further details on the design of the DNA carriers, their characterisation; modelling results on the field distribution in the nanopipette and on the binding equilibrium between the DNA capture probe and the carrier; additional nanopore translocation data at Vbias = 0.5 V; and further discussion of the statistical tests, including the 3-way ANOVA.

1) DNA design and characterisation

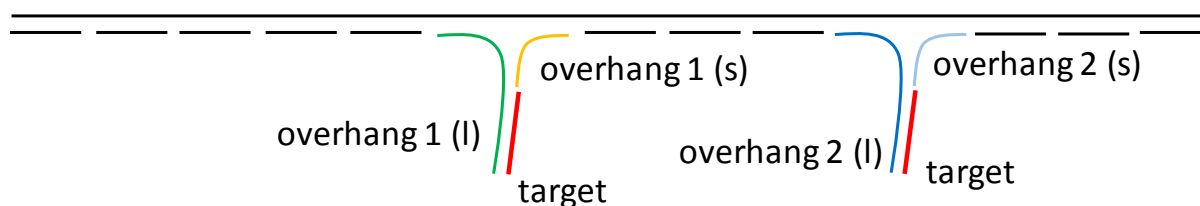DNA sequences used in the overhang region and illustration of the design:

Figure S1: Illustration of the DNA design with focus on the overhang regions, for ssx2/hyx2 (ssx1/hyx1 only contain overhang 1). The overall length of the overhangs is 100 nt, where the 12 nt closest to the carrier are hybridised (i.e., between overhang 1 (l) and overhang 1 (s), and overhang 2 (l) and overhang 2(s), respectively) to form a 'stalk' and stabilise the region. The remaining 88 nt of overhangs 1 (l) and 2 (l) act as probe and are complementary to the target.

Overhang 1 (s): 5' - ACT CCG ACC GAG CGC TGC TGC TTT CGG CGC CAG TAG CAC CAT TAC CAT TAG CAA GGC CGG AAA CGT CAC C – 3'; **overhang 1 (l)**: 5' - CTT GAG CCA TTT GGG AAT TAG AGC CAG CAA AAT CAC CAT GGC GCC GAA AGC AGC AGC GCT CGG TCG GAG TAT GCC CGA AAC GCC TAC CGG CGA TGT ACT GAC AAT CAG CAG TCC GGC ATT CGC CGA CGG TGC GCC GAT CCC GGA ACA GTA CAC CTG CA– 3'; **overhang 2 (s)**: 5' - TCG CTG GCA GCG TAC CGC GGC GGT CTG AGC CGT AGT GGC AAA TCC AAT CGC AAG ACA AAG AAC GCG AGA A – 3'; **overhang 2 (l)**: 5' - CTC CGG CTT AGG TTG GGT TAT ATA ACT ATA TGT CAC TAC GGC TCA GAC CGC CGC GGT ACG CTG CCA GCG AAT GCC CGA AAC GCC TAC CGG CGA TGT ACT GAC AAT CAG CAG TCC GGC ATT CGC CGA CGG TGC GCC GAT CCC GGA ACA GTA CAC CTG CA– 3'; **target**: 5' - TGC AGG TGT ACT GTT CCG GGA TCG GCG CAC CGT CGG CGA ATG CCG GAC TGC TGA TTG TCA GTA CAT CGC CGG TAG GCG TTT CGG GCA T– 3'

Below we show some further examples of AFM images of hyx1, cf. figure 2 in the main manuscript. In some cases, the overhang is easily identified, by visual inspection. In other cases, height information had to be taken into account as well, for example to rule out artefacts from DNA knots or coiling, as described in the Methods section of the main manuscript.
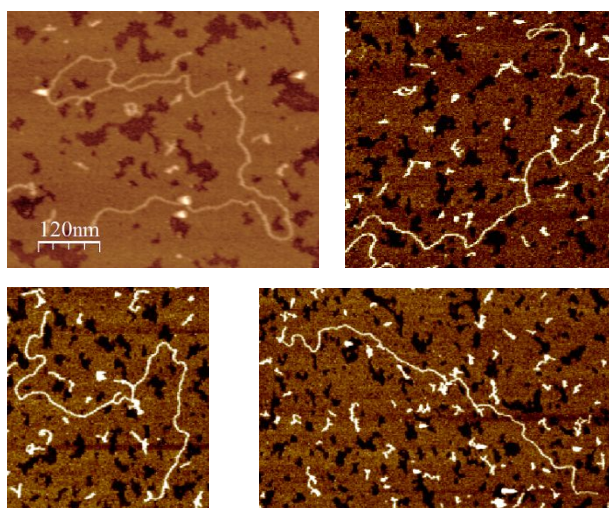
Figure S2: AFM imaging of the hyx1 construct, further examples.

DNA sample	First segment length [nm]	Overhang length [nm]	Second segment length [nm]	Total length [nm] (wo. overhang)
1	979	29.6	903	1882
2	903	50.8	1064	1967
3	922	38.8	981	1903
4	895	34.8	990	1885
5	760	45	778	1538
6	859	34.4	906	1765
7	970	39.2	972	1942
8	955	31	899	1854
9	853	25.9	830	1683
10	966	36.4	765	1731
11	725	42.1	951	1676
12	1090	47	849	1939
13	971	44.1	952	1923
14	839	46.8	1010	1849
15	818	24.8	796	1614
16	1210	48	717	1927
17	881	45	887	1768
18	766	31	983	1749
19	1116	42.7	703	1819
20	1020	32	897	1917
21	955	71.7	934	1889
22	979	36.6	673	1652
23	816.5	40.5	777	1593.5
Average:		39.2		1849

Table TS1: Length data forming the basis of the histograms shown in figure 2C in the main manuscript. Sample 1 is shown in figure 2B, samples 14-17 are shown in figure S2 above.

Thermodynamics of binding between overhang and target strands:

In order to confirm that the target sequence indeed bound to the probe with high enough efficiency, we calculated the concentration conditions based on thermodynamic, equilibrium binding considerations for the ssx1/hyx1 samples. For this purpose, we used the on-line implementation of OligoCalc with the 88 nt target sequence given above,[1] determined the Gibbs free energy of binding,

$$\Delta G = R \cdot T \cdot \ln\left(\frac{[\text{hyx1}]}{[\text{ssx1}] \cdot [\text{target}]}\right) = 634 \frac{\text{kJ}}{\text{mol}} \tag{S1}$$

and finally calculated the solution concentrations of the relevant species (T = 298 K), figure S3.

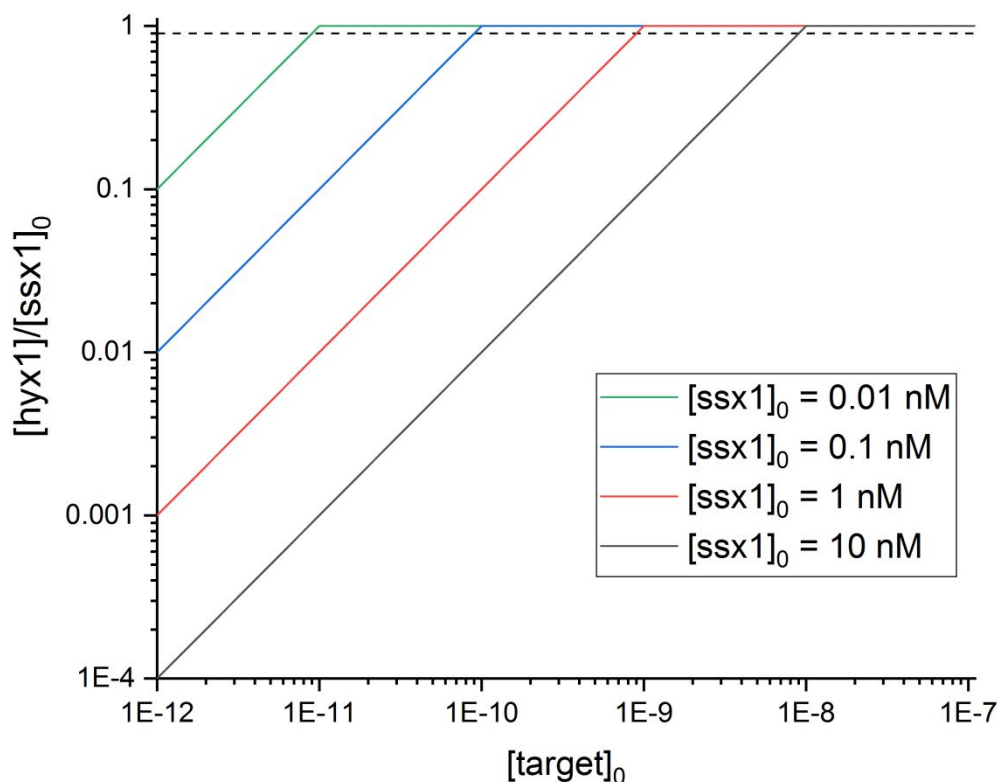**Figure S3**: The concentration of hyx1, [hyx1], relative to the initial concentration of ssx1, $[\text{ssx1}]_0$, as a function of the initial target concentration, $[\text{target}]_0$. $[\text{ssx1}]_0$ was varied, as indicated. Dashed line: $[\text{hyx1}]/[\text{ssx1}]_0 = 0.9$. Calculations were performed using eq. S1b, which has been re-arranged from eq. S1 with x = [hyx1], [target] = $[\text{target}]_0$ - x and so forth. The plot illustrates that the limit of detection, in terms of $[\text{target}]_0$, may be adjusted via $[\text{ssx1}]_0$. Considerations for ssx2 and hyx2 are similar, bearing in mind that there are now two, most likely independent binding sites.

$$[hyx1] = \frac{A \cdot ([ssx]_0 + [target]_0) - B + 1}{2A} \tag{S1b}$$

where $A = \exp(\Delta G/(RT))$ and $B = \sqrt{A^2 \cdot ([ssx]_0 - [target]_0)^2 + 2A \cdot ([ssx]_0 - [target]_0) + 1}$.

Gel electrophoresis results for some of the carrier constructs and other samples, as described:
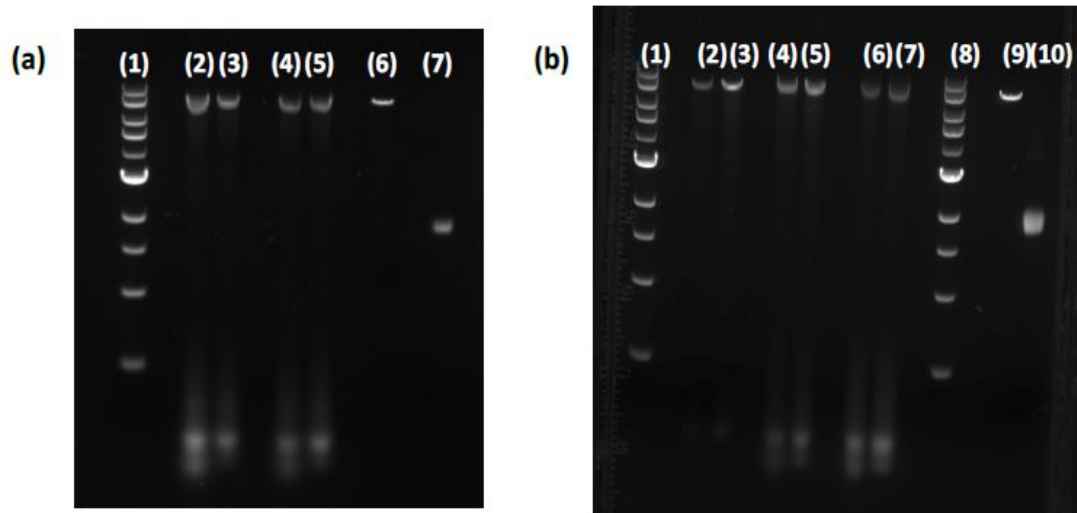

Figure S4: Gel shift assays of the carrier constructs and other samples as specified. a) Row 1: 1 kb ladder; 2/4: hyx1 before purification; 3/5: hyx1 after purification; 6: linearised ds M13mp18 DNA; 7: circular ss M13mp18 DNA. b) Row 1: 1 kb ladder; 2/3: ssx1 before/after purification; 4/5: ssx2 before/after purification; 6/7: hyx2 before/after purification; 8: 1 kb ladder; 9: linearised ds M13mp18 DNA; 10: circular ss M13mp18 DNA. Purification was performed with Amicon Ultra 100 kDa cut-off centrifugal filters, as described in the main text.

2) Conductance measurements and an estimation of the sensing zone

Electrode preparation: Ag wire (diameter: 0.25 mm; length: 7.1 cm, Goodfellow Cambridge Ltd, UK) was first cleaned by immersion in 34 % nitric acid (VWR International, Pennsylvania, USA) for 15 s. AgCl was deposited in 1 M KCl electrolyte (VWR International) with chronopotentiometry (I = 0.5 mA for 500 s). The Ag/AgCl electrodes were then soldered to gold pins to connect to the nanopore translocation set-up. The electrolyte solution was either 1 M KCl with TE buffer (10 mM Tris-HCl, 1 mM EDTA, pH 7.8, Sigma Aldrich) or 4 M LiCl with 10 mM TE, as specified. The electrolytes were filtered using a 0.2 μm syringe filter (EMD Millipore) to remove any large particle contaminants and then autoclaved. The nanopipette was back-filled with the electrolyte using a syringe needle (MicroFil, World Precision Instruments, Florida, U.S.A.) attached to a 1 mL syringe (NormJect Luer, Henke Sass Wolf, Germany). Air bubbles trapped in the nanopipette tip were removed by rasping with the corrugated end of a pair of tweezers. Glass vials used to contain the electrolyte (3 mL) were first sonicated in EtOH (VWR International) (2 rounds, 10 min. each) and then in ultrapure H_2O (3 rounds, 10 min. each) before leaving them to dry in an oven. They were then autoclaved for sterilisation prior to use.

The conductance of the nanopipette was determined from the slope of the I/V trace at low voltage in electrolyte (1 M KCl, 10 mM Tris-HCl, 1 mM EDTA or 4 M LiCl, 10 mM Tris-HCl, 1 mM EDTA) using cyclic voltammetry (Gamry Reference 600 Potentiostat, scan rate: 0.1 V/s, 2-electrode configuration), recorded in a potential range from +0.5 V to -0.5 V. The inner diameter d_p of the pipette tip was then estimated using the following equation:[2]

$$d_p = \frac{4GL + \frac{\pi}{2}GD_i}{\pi D_i g - \frac{\pi}{2}G} \tag{S2}$$

where G is the conductance and L the taper length of the nanopipette, D_i the inner diameter of the capillary (0.5 mm in our case), and g is the conductivity of the electrolyte (as measured with conductivity meter (Mettler-Toledo, Greifensee, Switzerland). The taper lengths of all the pipettes used were measured by optical microscopy (Olympus, Tokyo, Japan) from the tip of the capillary to where the internal channel had reached D_i. The values obtained corresponded rather well to those obtained from SEM and TEM imaging, which was performed on a small selected number of pipettes. As discussed in the main text, the channel geometry is close to conical even rather far along the pipette and away from the tip. Since the pore diameter increases accordingly, the contribution to the overall resistance of the decreases markedly. The resistance of a conical pipette is given by

$$R = \frac{\rho}{\pi} \cdot \frac{L_c}{r_{in} \cdot r_{out}} \tag{S3}$$

where ρ is the resistivity of the solution, $\rho = 1/g$; L_c the axial length of the conical channel; and r_{in} and r_{out} the pore radii at the entrance and exit of the channel. It can then be shown the resistance of a conical pore of length L_c', relative to one of length L_c, is (with $L_c' \leq L_c$):

$$\frac{R(L_c')}{R(L_c)} = \frac{L_c' \cdot (L_c \cdot tan(\alpha) + r_{in})}{L_c \cdot (L_c' \cdot tan(\alpha) + r_{in})} \tag{S4}$$

α is the opening angle of the cone, relative to the pore axis.

This relation is plotted in figure S5 below. It demonstrates that even within the first 10 nm from the pore entrance, almost 20% of the resistance drop occur. After 100 nm, this resistance drop already exceeds 70%. Thus, the sensing zone, i.e. the region that is most sensitive to changes in resistance lies within the first few 10s of nanometers from the pipette tip.
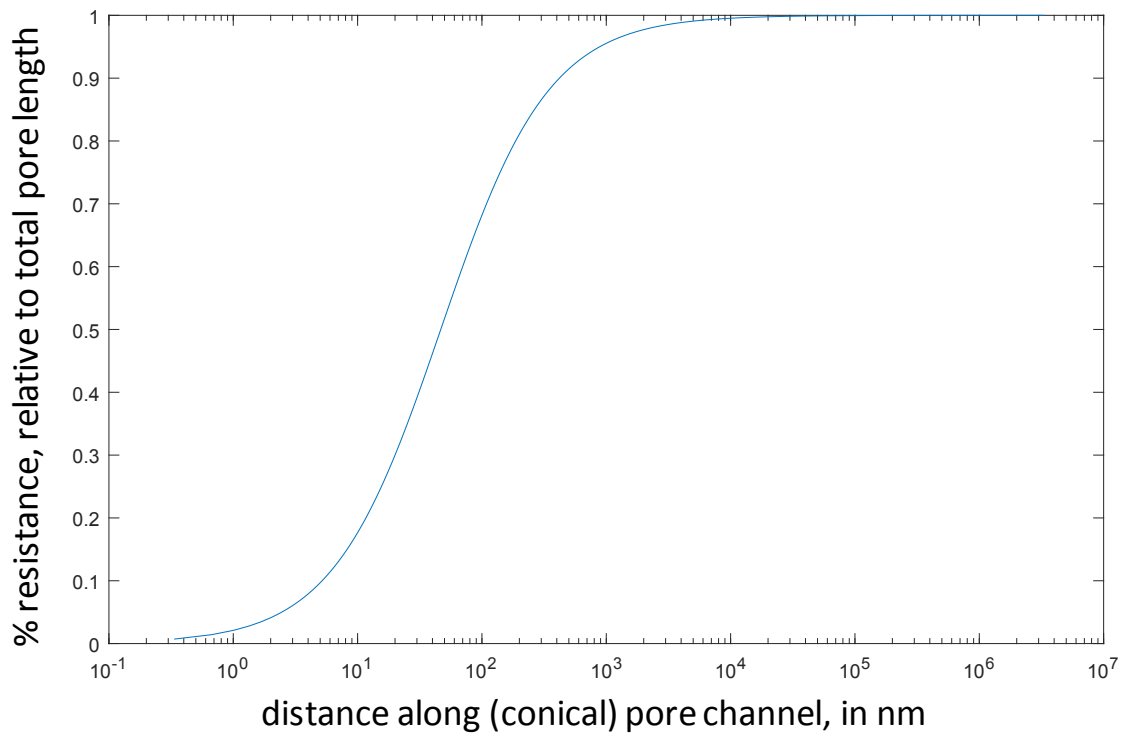

Figure S5: Relative resistance of a conical pore as a function of L_c', at given L_c, according to eq. S4. Opening angle $\alpha = 15°$; membrane thickness $L_c = 3.35$ mm; pore radius, entry side: $r_{in}=12.5$ nm. The figure illustrates the relative contribution to the overall resistance of the pore, as the distance L_c' along the pore channel is increased (counted from the pore entrance).

3) DNA knotting

It has been reported previously that even translocation of bare double-stranded DNA can produce current-time transients including a 'spike-like' feature, for example due to knotting.[3] Spikes resulting from the latter are typically roughly three times larger than the current level associated with linear ds DNA, due to the geometry of the knot. Since similar spike features are an important aspect in our study as well, we wanted to understand whether they occur and how abundant they are in our case, ultimately to rule out artefacts in the interpretation of our core results. For this purpose, translocation experiments were performed with 7.2 kbp (ds) M13mp18 DNA that did not contain any overhangs. Indeed, some events resembled the pattern expected for DNA knots, as shown in figure S6. It turned out, however, that they were rather rare and occurred in only 3.1% of 820 translocation events, in line with the previous literature (4.4 % in ref. 3). We therefore felt that their presence would not seriously affect the experiments with the overhang-containing samples and did not make any attempts to separate them out in those datasets.
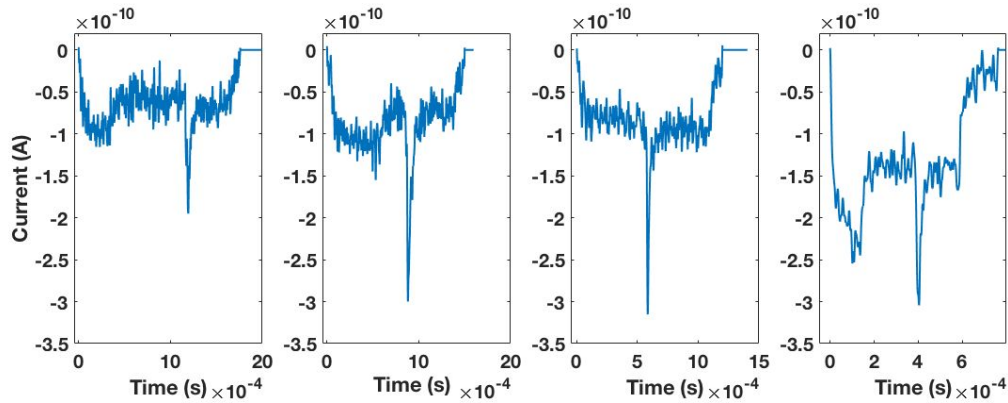

Figure S6: Example events from the translocation of 7.2 kbp M13mp18 DNA at different V_{bias} (0.3 V; 0.5 V; 0.5 V and 0.7 V from left to right (4 M LiCl electrolyte; d_p = 19 nm; 100 kHz filter frequency)

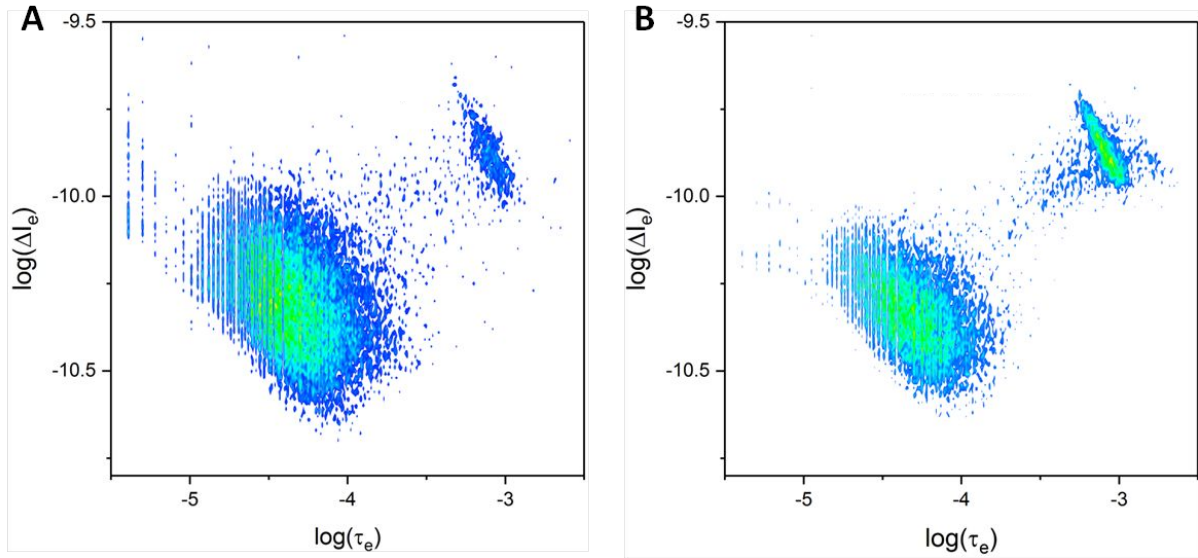## 4) Comparison of translocation data for hyx1 and ssx1

Figure S7: Comparison of translocation data for hyx1 (A) and ssx1 (B). The data in panel A are from three different pipettes (59964 events in total), as described in the main manuscript; those in panel B from four pipettes (29776 events in total). DNA fragments are seen in both cases, in the larger cluster (bottom left), while the DNA carrier forms a smaller, separate cluster (top right). The translocation characteristics for the two samples, and in particular the event cluster, are virtually the same, suggesting that hybridisation of the overhang does not influence the translocation of the carrier significantly.

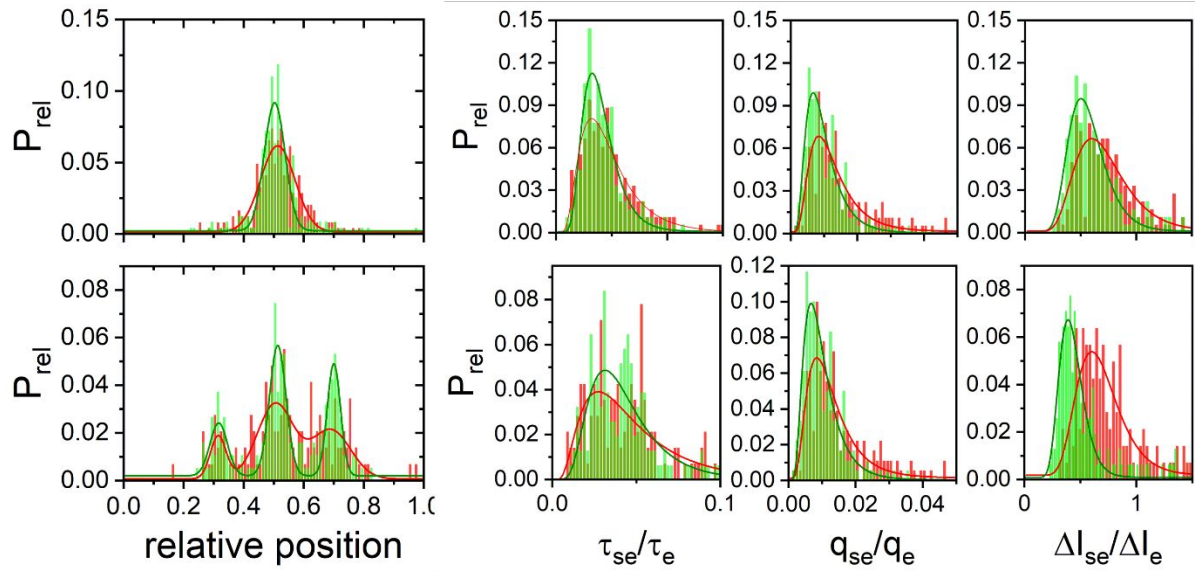**5) Sub-event translocation data for V_{bias} = 0.5 V**

Figure S8: DNA carrier translocation data, analysis of sub-events (V_{bias} = 0.5 V). The arrangement and color-coding is the same as in figure 4 of the main text, namely ssx1/hyx1 (top) and ssx2/hyx2 (bottom). ssx samples in green, hyx in red. Left: Normalised histograms of the relative sub-event position for single-overhang samples (top) and the double-overhang samples (bottom), inc. Gaussian fits. Right: Normalised histograms of sub-event characteristics, relative to the respective event: τ_{se}/τ_e, q_{se}/q_e and $\Delta I_{se}/\Delta I_e$. All distributions are non-Gaussian and are represented well by log-normal fits (solid lines). As for V_{bias} = 0.7 V, the largest difference between the ssx and hyx samples appears to be in the $\Delta I_{se}/\Delta I_e$ distributions, which were then used for further analysis. We note that the experiments at different V_{bias} were performed in different pipettes, so the data from the two voltage conditions are independent.

6) Results of normality testing (Kolmogorov-Smirnow (K.S.) test)

Sample	DF	Statistic	p-value	Decision at level (5%)
hyx1, 0.7 V	367	0.05602	0.19736	Can't reject normality
ssx1, 0.7 V	496	0.07127	0.01271	Reject normality
hyx1, 0.5 V	181	0.06954	0.34066	Can't reject normality
ssx1, 0.5 V	180	0.05942	0.55318	Can't reject normality
hyx2, 0.7 V	399	0.03701	0.66657	Can't reject normality
ssx2, 0.7 V	435	0.06116	0.07606	Can't reject normality
hyx2, 0.5 V	141	0.08594	0.24187	Can't reject normality
ssx2, 0.5 V	155	0.10657	0.05654	Can't reject normality

Table TS2: Results from the K.S. test for the individual samples. 'DF': Degrees of Freedom; 'Statistic': K.S. test statistic. Normality is only formally rejected in one case, ssx1 at V_{bias} = 0.7 V.
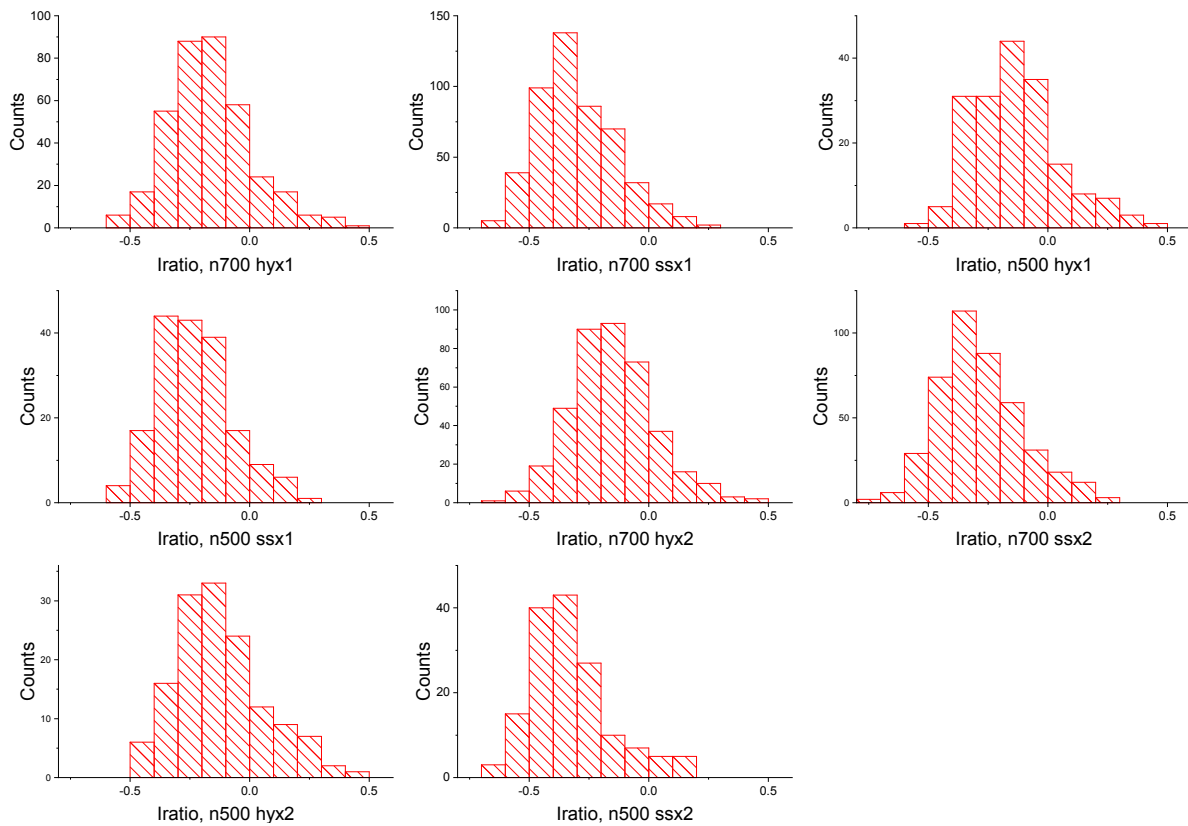
Figure S9: log($\Delta I_{se}/\Delta I_e$) histograms for the individual samples. Despite log-transformation, they still are slightly asymmetric. However, given that ANOVA is known to be rather robust towards non-normality, this does not (significantly) affect the conclusions form the analysis.
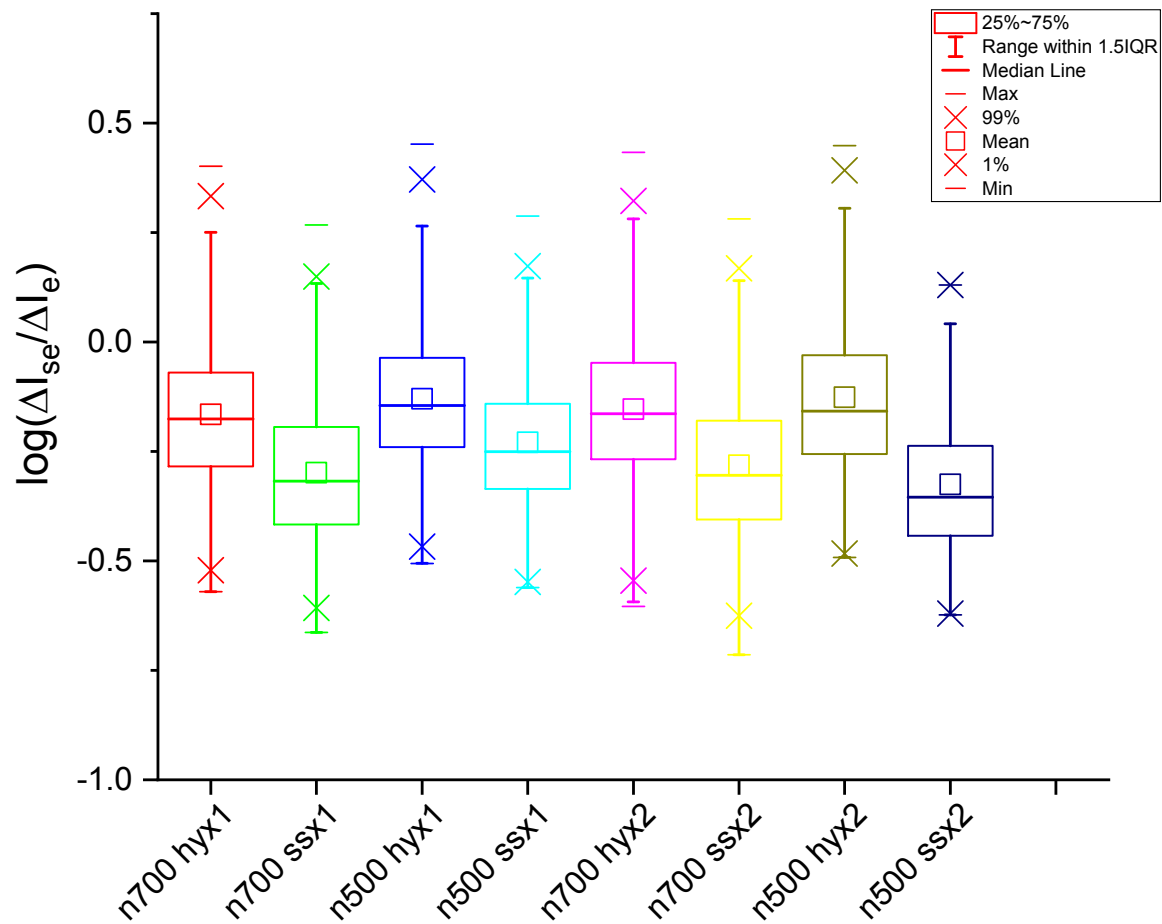

Figure S10: Box plot corresponding to the datasets shown above.

7) Further discussion of the ANOVA results, main and interaction effects

Conventional ANOVA has several requirements, namely that the data be (approximately) normally distributed, possess equal (or comparable) variance and be independent. The latter is the case here, since the individual datasets were recorded in separate experiments in several (23) different pipettes. ANOVA is relatively robust with regards to data that are not normally distributed, but in light of the results shown in figure 4 C) (log-normally distributed data), the $\Delta I_{se}/\Delta I_e$ data were log-transformed first. A Kolmogorov-Smirnov test was then performed to check for normality (cf. SI). In all eight cases (datasets for ssx1, hyx1, ssx2 and hyx2 at V_{bias} = 0.5 V and 0.7 V, respectively) the distributions appeared close to normal, only for one dataset was normality formally rejected at a confidence level of 0.05 (ssx1 at V_{bias} = 0.7 V, p = 0.013). A Levène test was performed to compare the variances of the different distributions, which were found to be not significantly different at a confidence level of 0.05. As a result, we felt the requirements for an ANOVA were sufficiently fulfilled to proceed with the analysis.

The results of the three-factor ANOVA are shown in figure S11 below, according to the three factors from top to bottom. The black squares represent the mean values of $\log(\Delta I_{es}/\Delta I_e)$, the individual data points for each set are shown as colormaps (white/blue: low/high density). The means of the first two factors, 'hybridisation state' and 'voltage', are significantly different at a 0.05 confidence level (p ≈ 0 and 0.008; means difference: -0.139 and 0.021; sample sizes: 1266/1088 and 657/1697), while the third one, 'number of overhangs', is not (p = 0.061; means difference: 0.015; sample size: 1224/1130). We note that the sample sizes are approximately equal in most cases, except for the effect of 'voltage'. The latter does not seem to affect the homogeneity of variance test and is thus unlikely to affect the conclusions of the ANOVA in this regard. Notably, the first observation is of significant interest in that it seems to support the underlying idea of the present work. However, the interpretation of these main effects is only straightforward in the absence of significant interaction terms. Such interaction terms represent the effect of one factor on another one, for example if there were a significant difference between ssx and hyx for one V_{bias} value, but not for another one. In that case, V_{bias} would have to be considered explicitly, in order to make a statement regarding the statistical significance of the difference between ssx and hyx (and so forth). In the presence of significant interaction, suitable *post hoc* tests are needed to explore the relation between different sub-groups, as we show in the main text. The overall ANOVA results are tabulated below.

Accordingly, at the 0.05 confidence level, we found two significant 'first-order' interactions, namely between 'voltage' and 'number of overhangs' ('Voltage·#sub-ev.'; F-value: 13.71; P-value: $2.177 \cdot 10^{-4}$) and 'hybridisation state' and 'number of overhangs' ('sample·#sub-ev.'; F-value: 9.980; P-value: 0.0016), respectively. In the first case, this would suggest that the statistical significance of the difference in the $\log(\Delta I_{se}/\Delta I_e)$ distributions between single- and double-overhang samples could depend on voltage. From a sensing point of view, it is clearly desirable for there to be no interaction with the number of overhangs, because it implies that then they are detected independently from each other. Equally, in the second case, the result suggests that depending on the number of overhangs, the statistical significance in differentiating ssx from hyx samples may vary.

	DF	Sum of Squares	Mean Square	F Value	P Value	Sig
Voltage	1	0.2052	0.2052	7.080	0.0079	1
Sample	1	9.0035	9.0035	310.666	0	1
#sub-ev.	1	0.1016	0.1016	3.506	0.0613	0
Voltage·Sample	1	0.0290	0.0290	0.9999	0.3175	0
Voltage·#sub-ev.	1	0.3975	0.3975	13.714	2.177E-4	1
Sample·#sub-ev.	1	0.2892	0.2892	9.9797	0.0016	1
Voltage·Sample·#sub-ev.	1	0.3459	0.3459	11.935	5.606E-4	1
Model	7	11.834	1.6906	58.335	0	
Error	2346	67.990	0.0290	0	0	
Corrected Total	2353	79.824	0	0	0	

Table TS3: ANOVA results table (overall). Significant interaction are labelled '1' in the last column.

Starting with the interaction between 'voltage' and 'number of overhangs', it is apparent from the table below that the difference between ssx and hyx samples is statistically significant for V_{bias} = 0.5 V (at the 0.05 level; means difference = +0.0438), while at V_{bias} = 0.7 V it is not (means difference = -0.0144). Thus, the reason why the main effect of 'number of overhangs' (single vs. double) is not found to be statistically significant, is most likely due to the partial cancellation of the means differences between different datasets. More detailed investigation further reveals that in fact only the difference between ssx1 and ssx2 at V_{bias} = 0.5 V is statistically significant (means difference: +0.0959), while hyx1 vs. hyx2 at V_{bias} = 0.5 V, and ssx1 vs. ssx2 and hyx1 vs. hyx2 at V_{bias} = 0.7 V are not (means differences: -0.0082; -0.0167; -0.0121, respectively). Therefore, at the individual level there does not seem to be a consistent statistically significant difference between the single and double-overhang samples, in line with the overall main effect.

A slightly different picture emerges for the second observed interaction, namely between 'hybridisation state' and 'number of overhangs'. A subset of the underlying direct comparisons, namely ssx1 vs. hyx1 and ssx2 vs. hyx2, represent the core of the present study and are discussed in detail in the main text. The other comparisons, ssx1 vs. hyx2 and ssx2 vs. hyx1, also yield statistically significant differences, but in absence of a statistically significant effect from the number of

overhangs, they simply reflect differences in hybridisation state. In the context of the present study, they are less relevant, as we aim to determine the hybridisation state of a given DNA structure.
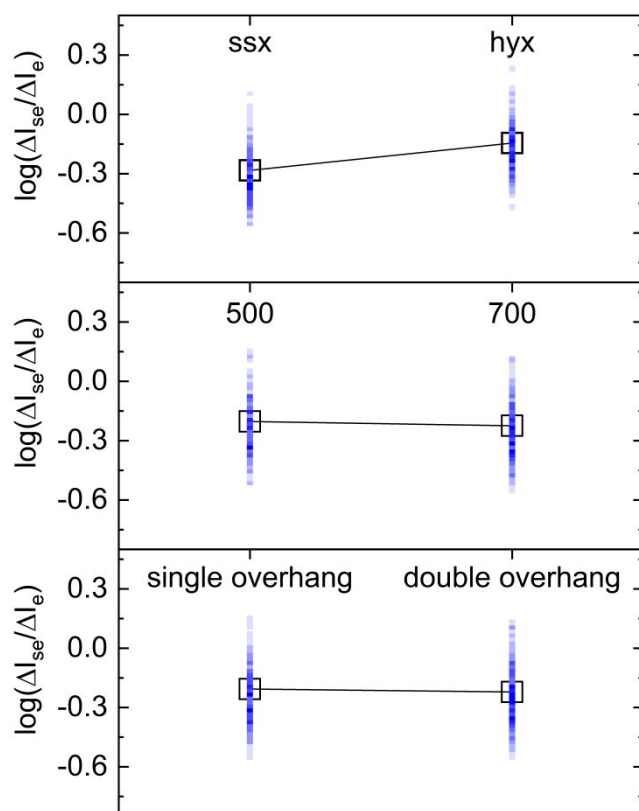
Figure S11: Results for a 3-way ANOVA on the log-transformed $\Delta I_{se}/\Delta I_e$ data. The factors and levels were the hybridisation state ('ssx', 'hyx'; top), the voltage (500 mV, 700 mV; middle) and the number of overhangs/ protrusions on the DNA carrier ('single', 'double'; bottom). Black squares: Mean values. Colormaps: Histograms of the individual log($\Delta I_{se}/\Delta I_e$) values with blue and white corresponding to high and low density, respectively. The means of the first two factors are significantly different at a 0.05 confidence level (p = 0 and 0.008), while the third is not (p = 0.061). See main text for further discussion.
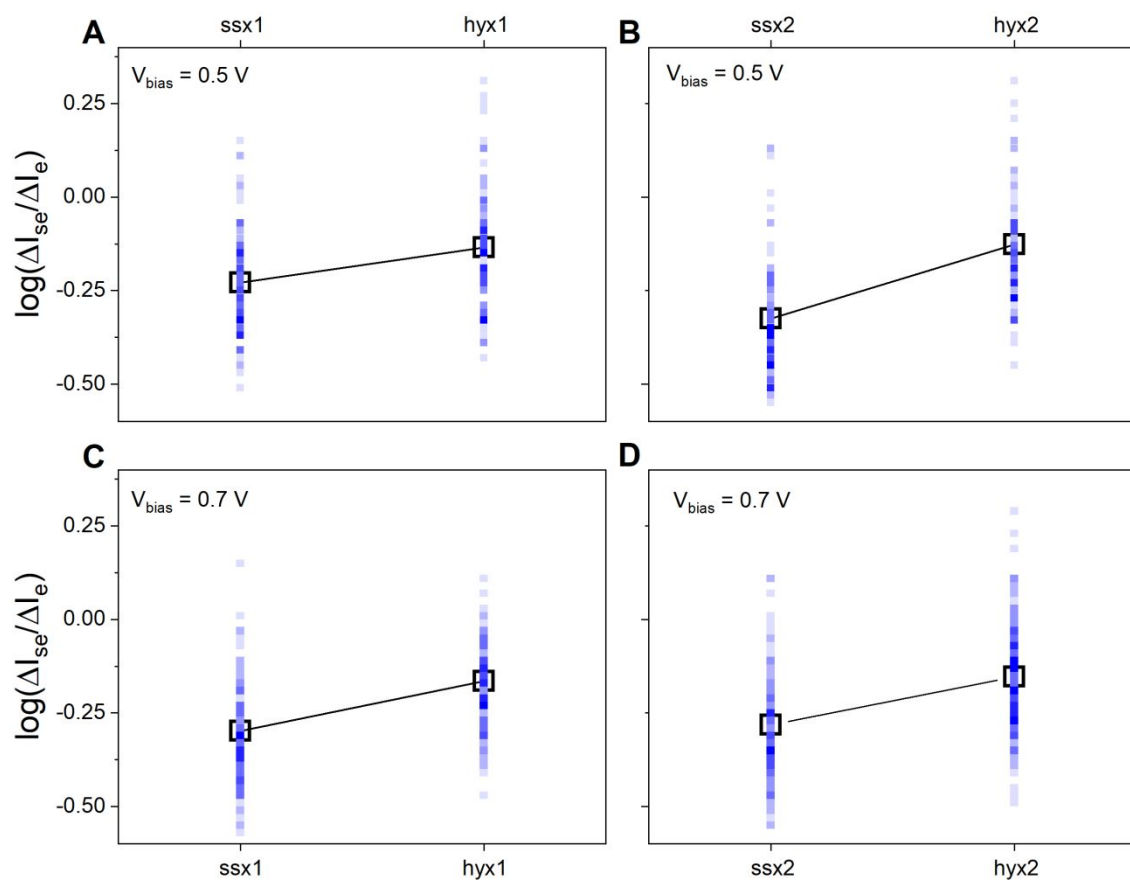
Figure S12: Result of the pair-wise comparisons ssx1 vs. hyx1 and ssx2 vs. hyx2 at V_{bias} = 0.5 V (A/B) and 0.7 V (C/D). The respective mean values (black squares) and individual data points (density maps, blue/white: high/low density) are shown. The means difference is comparable in magnitude in each case and such that $\log(\Delta I_{se}/\Delta I_e)$ is consistently larger for hyx samples, compared to the corresponding ssx samples (see main text for further discussion).

Voltage	Sample	#sub-ev.	Voltage	Sample	#sub-ev.	MeanDiff	SEM	q Value	Prob	Sig
500	ssx	--	500	hyx	--	-0.14653	0.01333	-15.541	2.22E-16	1
500	ssx	--	700	ssx	--	0.01307	0.01086	1.702	0.62	0
500	ssx	--	700	hyx	--	-0.11773	0.01116	-14.924	2.22E-16	1
500	hyx	--	700	ssx	--	0.1596	0.01106	20.413	2.22E-16	1
500	hyx	--	700	hyx	--	0.0288	0.01135	3.588	0.05	0
700	ssx	--	700	hyx	--	-0.1308	0.0083	-22.280	2.22E-16	1
500	--	single	500	--	double	0.04387	0.01333	4.652	0.00554	1
500	--	single	700	--	single	0.05007	0.01069	6.625	1.67E-5	1
500	--	single	700	--	double	0.03567	0.01071	4.709	0.0048	1
500	--	double	700	--	single	0.0062	0.01149	0.763	0.9493	0
500	--	double	700	--	double	-0.0082	0.01151	-1.008	0.8922	0
700	--	single	700	--	double	-0.0144	0.0083	-2.453	0.3055	0
--	ssx	single	--	ssx	double	0.03958	0.01086	5.157	0.0015	1
--	ssx	single	--	hyx	single	-0.11381	0.01069	-15.0590	2.220E-16	1
--	ssx	single	--	hyx	double	-0.12393	0.01113	-15.741	2.220E-16	1
--	ssx	double	--	hyx	single	-0.1534	0.01108	-19.580	2.220E-16	1
--	ssx	double	--	hyx	double	-0.16352	0.01151	-20.090	2.220E-16	1
--	hyx	single	--	hyx	double	-0.01012	0.01135	-1.261	0.809	0
500	ssx	single	500	ssx	double	0.0959	0.01862	7.283	7.218E-6	1
500	ssx	single	500	hyx	single	-0.0945	0.01789	-7.471	3.534E-6	1
500	ssx	single	500	hyx	double	-0.10267	0.01911	-7.597	2.167E-6	1
500	ssx	single	700	ssx	single	0.06938	0.01479	6.635	7.377E-5	1
500	ssx	single	700	ssx	double	0.05265	0.01506	4.944	0.011	1
500	ssx	single	700	hyx	single	-0.06374	0.01546	-5.829	9.807E-4	1
500	ssx	single	700	hyx	double	-0.07582	0.01526	-7.027	1.853E-5	1
500	ssx	double	500	hyx	single	-0.1904	0.0186	-14.478	4.441E-16	1
500	ssx	double	500	hyx	double	-0.19856	0.01978	-14.198	4.441E-16	1
500	ssx	double	700	ssx	single	-0.02652	0.01564	-2.398	0.690	0
500	ssx	double	700	ssx	double	-0.04325	0.0159	-3.847	0.116	0
500	ssx	double	700	hyx	single	-0.15964	0.01628	-13.868	4.441E-16	1
500	ssx	double	700	hyx	double	-0.17172	0.01609	-15.098	4.441E-16	1
500	hyx	single	500	hyx	double	-0.00817	0.01909	-0.605	0.9999	0
500	hyx	single	700	ssx	single	0.16388	0.01476	15.704	4.441E-16	1
500	hyx	single	700	ssx	double	0.14715	0.01503	13.844	4.441E-16	1
500	hyx	single	700	hyx	single	0.03076	0.01544	2.818	0.487	0
500	hyx	single	700	hyx	double	0.01868	0.01523	1.734	0.924	0
500	hyx	double	700	ssx	single	0.17205	0.01622	15.001	4.441E-16	1
500	hyx	double	700	ssx	double	0.15532	0.01647	13.337	4.441E-16	1
500	hyx	double	700	hyx	single	0.03892	0.01684	3.269	0.287	0
500	hyx	double	700	hyx	double	0.02684	0.01665	2.280	0.743	0
700	ssx	single	700	ssx	double	-0.01673	0.01116	-2.119	0.809	0
700	ssx	single	700	hyx	single	-0.13313	0.0117	-16.089	4.441E-16	1
700	ssx	single	700	hyx	double	-0.1452	0.01143	-17.967	4.441E-16	1
700	ssx	double	700	hyx	single	-0.1164	0.01205	-13.665	4.441E-16	1
700	ssx	double	700	hyx	double	-0.12847	0.01178	-15.423	4.441E-16	1
700	hyx	single	700	hyx	double	-0.01208	0.01229	-1.390	0.977	0

Table TS4: ANOVA results table of interaction effects (α = 0.05 in all cases).

References

[1] W.A. Kibbe, OligoCalc: an online oligonucleotide properties calculator, Nucl. Acids Res. 2007, 35, W43-W46.

[2] L.J. Steinbock, A. Lucas, O. Otto, U.F. Keyser, Voltage-driven transport of ions and DNA through nanocapillaries, Electrophoresis, 2012, 33, 3480-3487.

[3] C. Plesa, D. Verschueren, S. Pud, J. van der Torre, J.W. Ruitenberg, M.J. Witteveen, M.P. Jonsson, A.Y. Grosberg, Y. Rabin, C. Dekker, Direct observation of DNA knots using a solid-state nanopore, Nat. Nanotechnol. 2016, 11, 1093-1097.